European Heart Journal (2012) **33**, 16–25
doi:10.1093/eurheartj/ehr384

CURRENT OPINION

From metallic cages to transient bioresorbable scaffolds: change in paradigm of coronary revascularization in the upcoming decade?

Patrick W. Serruys*, Hector M. Garcia-Garcia, and Yoshinobu Onuma

Thorax Centrum, Erasmus MC, 's Gravendijkwal 230, 3015 CE Rotterdam, The Netherlands

Received 28 June 2011; revised 22 August 2011; accepted 26 September 2011; online publish-ahead-of-print 31 October 2011

This paper was guest edited by Antonio Colombo, Cardiac Catheterization Laboratory, EMO GVM Centro Cuore Columbus, Milan, Italy

1977, 1986, 1999

Drug-eluting bioresorbable scaffolds (BRSs) may in the near future change drastically the landscape of percutaneous coronary revascularization.[1] In 1977, when Andreas Gruentzig introduced the concept of percutaneous transluminal coronary angioplasty, the most feared enemy of the operators was acute occlusion of the dilated lesion due to a combination of elastic recoil and intimal and medial dissection, sometimes aggravated by intraparietal haematoma (*Figure 1*).[2] Surgical standby was a *sine qua non* condition for the safe performance of the percutaneous treatment. At short term, proliferative neointima and constrictive remodelling could dissipate the transient benefit of the therapeutic dilatation of the stenosis. However, in the case of favourable healing following the barotrauma, late lumen enlargement, plaque regression, and vessel remodelling could occur and be modulated by change in life style, preventive medicine, and pharmacological anti-atherosclerotic agents.[3]

In 1986, the introduction of metallic scaffolds was initially perceived as an *ad hoc* solution to the problem of acute vessel occlusion (*Figure 1*).[4–6] But the implantation of the metallic endoluminal prosthesis in a thrombogenic milieu was considered as a double-edged sword. ('The bailout stent. Is a friend in need always a friend indeed?'[7]) Nevertheless, scaffolding dissected post-balloon dilatation with a metallic mesh became an important safeguard in angioplasty. Furthermore, the recoil and constrictive remodelling appeared to be actively and efficiently counteracted, thereby reducing the frequency and the severity of the restenosis.[8] However, the implantation of a permanent foreign body created and generated a new iatrogenic disease: intra-stent restenosis.[9] The amount of neointima generated by the permanent implantation of a metallic scaffold was, as a matter of fact, larger than the one induced by the barotrauma of balloon angioplasty (loss following balloon angioplasty: 0.32 mm vs. loss following stent implantation: 0.65 mm).[10,11]

With the advent of stenting appeared on the scene new potentially fatal enemies: subacute and late stent thrombosis,[12] but eventually, the adoption of stenting in the field of angioplasty was perceived as a beneficial revolution. A decade later, in 1999, coating and elution of cytostatic and cytotoxic drugs from the stent surface set the stage for a new revolution by reducing, if not eliminating, the exuberant intra-stent neointima in response to the implantation of a foreign body[13–15] (*Figure 1*).

However, this new 'medicinal device' created again a new enemy: by interfering profoundly with the healing process, lack of endothelialization and late persistent or acquired malapposition of the permanent metallic implant became the nidus of late and very late stent thrombosis, without mentioning the hypersensitive reaction mediated by eosinophils that sometimes triggered these catastrophic events.[16–18]

Potential benefits of a transient scaffold

From the very early days, interventional cardiologists have been dreaming of a transient scaffold that would disappear 'after the job has been done' (*Figure 1*).[19,20] Percutaneous coronary intervention (PCI) with BRSs has potential advantages over the current generation metallic bare-metal stent (BMS)/drug-eluting stent (DES) technology. These include potential reductions in adverse events such as stent/scaffold thrombosis, as after bioresorption, there would potentially be no triggers for thrombosis, such as uncovered stent struts, durable polymer, or remnant drug. The absence of these foreign materials may also reduce the requirements for long-term dual antiplatelet therapy, resulting in the

* Corresponding author: Tel: +31 10 463 5260, Fax: +31 10 436 9154, Email: p.w.j.c.serruys@erasmusmc.nl

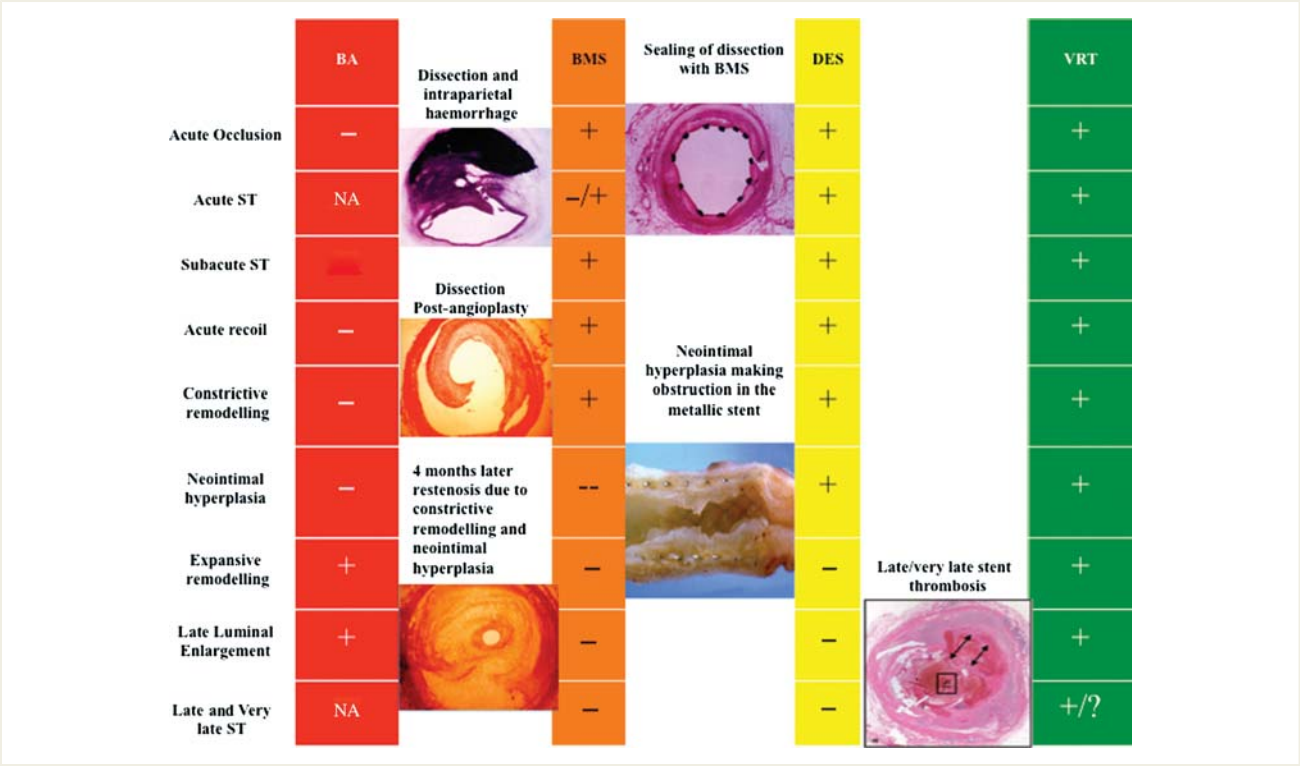

Figure 1 This schematic illustration depicts the evolution of percutaneous coronary revascularization from balloon angioplasty (BA), bare-metal stents (BMS), and drug-eluting metallic stents (DES) to vascular reparative therapy (VRT). '+' implies prevented or not restricted, while '−' implies not prevented, or restricted. NA, not applicable because of the absence of stent; ST, stent thrombosis.

potential reduction in associated bleeding complications. Physiologically, the absence of a rigid metallic cage can facilitate the restoration of the vessel vasomotor tone, adaptive shear stress, late luminal enlargement, and late expansive remodelling. In the long term, BRS should not hamper future treatment options such as PCI, CABG, or pharmacologically induced plaque regression. Bioresorbable scaffold may also be suitable for vascular anatomy where scaffolds are prone to crushing and fractures, as seen in the femoral or tibial arteries.[21]

Furthermore, BRS can obviate some of the other problems associated with the use of permanent metallic stents such as the covering of side branches.[22] Bioresorbable scaffold also appears to be suitable for non-invasive imaging such as computed tomographic angiography or magnetic resonance imaging, due to the absence of artefact caused by permanent metallic materials.[23,24]

In the early 1990s, scaffolds with biostable polymers were successfully tested in the porcine model by our group in Rotterdam.[25] The Igaki-Tamai stent was the first clinical attempt to use polylactide as a mechanical scaffold following balloon dilatation of stenotic lesions.[26] This pioneering device was implanted in seven patients in Rotterdam in 1999. The angiographic follow-up and optical coherence tomography (OCT) assessment of long-term results was performed in one of them during a live case demonstration at EuroPCR in 2009.[27] Although the long-term follow-up has clearly demonstrated the innocuousness of that specific polymer on the long-term architecture of the vessel wall, the restenosis rate in the first 6 months was comparable to that observed with BMSs[27–29] and the technology almost fell in desuetude. Recently, the use of polylactide scaffolds eluting everolimus has demonstrated the potential of that technology to treat stenotic lesion with transient scaffolds.[24,30,31] Other technologies using a resorbable metal such as magnesium alloy with elution of paclitaxel are currently undergoing testing (*Table 1*).[32] Other technologies using polymer other than polylactide are also being investigated.[33]

At first glance, physicians may not see the long-term implication of this change in technology. The two central schematic illustrations of this editorial attempt to sketch the potential change in paradigm that these new technologies will possibly bring in the coming decade (*Figures 2* and *3*).

From a permanent metallic cage . . .

The atherosclerotic process is characterized by a lumen reduction (vertical axis in *Figure 2*) associated with remodelling (horizontal axis in *Figure 2*) of the vessel wall delineated by the external elastic membrane (EEM). Glagov and other anatomopathologists have described this complex interaction between the growth of atherosclrelotic plaque, reduction in lumen, and compensatory enlargement of the external envelope of the vessel.[34] If intimal thickening (IT) is an early adaptative process, related to ageing, it may at certain point become pathological IT, and as its name indicates, be the initial stage of a morbid process that will ultimately result in an atherosclerotic plaque with fibrotic, fibrofatty tissue, dense calcium, and necrotic core.[35]

Table 1 **Summary of the clinically investigated bioresorbable scaffolds**

Scaffold	Strut material	Coating material	Design	Absorption products	Drug elution	Stent radio-opacity	Total strut thickness (strut + coating) (μm)	Crossing profile (mm)	Stent-to-artery coverage (%)	Duration radial support	Absorption time	Angiographic late loss	TLR rate
Igaki-Tamai	Poly-L-lactic acid	Nil	Zig-zag helical coils with straight bridges	Lactic acid, CO_2, and H_2O	Nil	Gold markers	170		24	6 months	2 years	Late loss index at 6 months: 0.48 mm	At 6 months: 6.7%
AMS-I	Metal—magnesium alloy	Nil	Sinusoidal in-phase hoops linked by straight bridges	Not applicable	Nil	Nil	165	1.2	10	Days or weeks	<4 months	At 4 months: 1.08 mm	At 1 year: 45%
AMS-II	Metal—magnesium alloy	Nil		Not applicable	Nil	Nil	125	—	—	Weeks	>4 months		
AMS-III	Metal—magnesium alloy	Nil		Not applicable	Paclitaxel	Nil	125	—	—	Weeks	>4 months	At 6 months: 0.68 mm	At 6 months: 9.1%
REVA	Poly-tyrosine-derived polycaronate polymer	Nil	Side and lock	Amino acid, ethanol, CO_2	Nil	Iodine impregnated	200	1.7	55	3–6 months	2 years	At 6 months: 1.81 mm	At 1 year: 67%
BTI	Polymer salicylate + linker	Salicylate + different linker	Tube with laser-cut voids	Salicylate, CO_2, and H_2O	Sirolimus salicylate	Nil	200	2	65	3 months	6 months		
BVS 1.0	Poly-L-lactide	Poly-D,L-lactide	Out-of-phase sinusoidal hoops with straight and direct links	Lactic acid, CO_2, and H_2O	Everolimus	Platinum markers	156	1.4	25		2 years	At 6 months: 0.44 mm	At 4 years: 0%
BVS 1.1	Poly-L-lactide	Poly-D,L-lactide	In-phase hoops with straight links	Lactic acid, CO_2, and H_2O	Everolimus	Platinum markers	156	1.4	25	6 months	2 years	At 6 months: 0.19 mm at 12 months: 0.27 mm	At 1 year: 3.6%

TLR, target lesion revascularization.

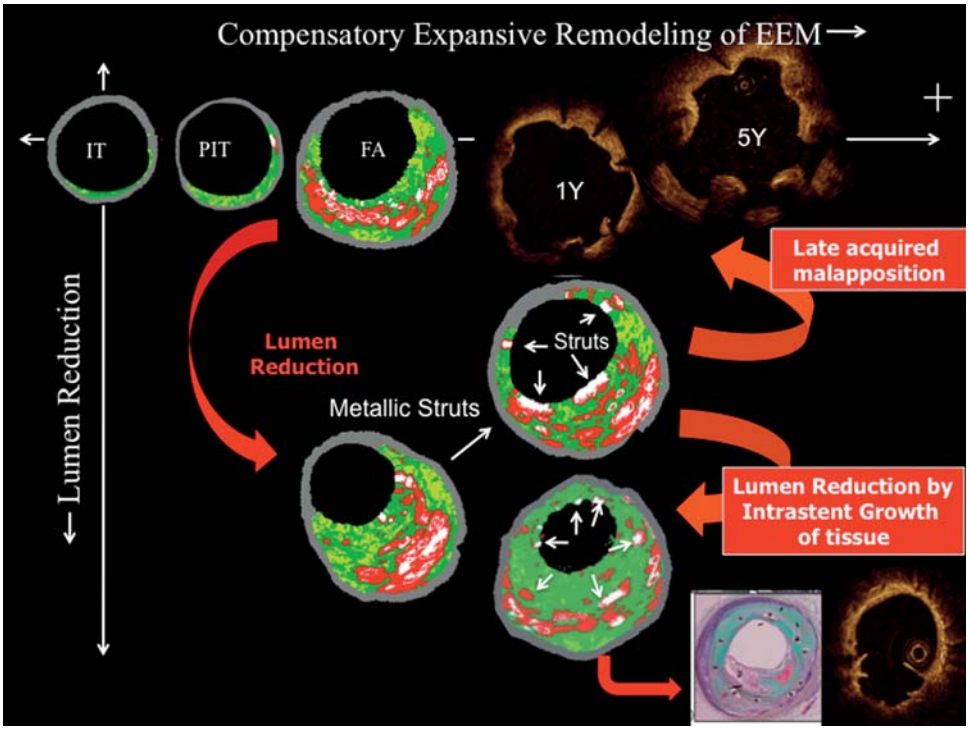

Figure 2 The atherosclerotic process is characterized by a lumen reduction (vertical axis) associated with remodelling (horizontal axis) of the vessel wall. Intimal thickening (IT) becomes pathological thickening (PIT), ultimately resulting in a fibroatheromatous plaque (FA) with fibrotic, fibrofatty, dense calcium, and necrotic core. Late evolutional events are fully described in the text.

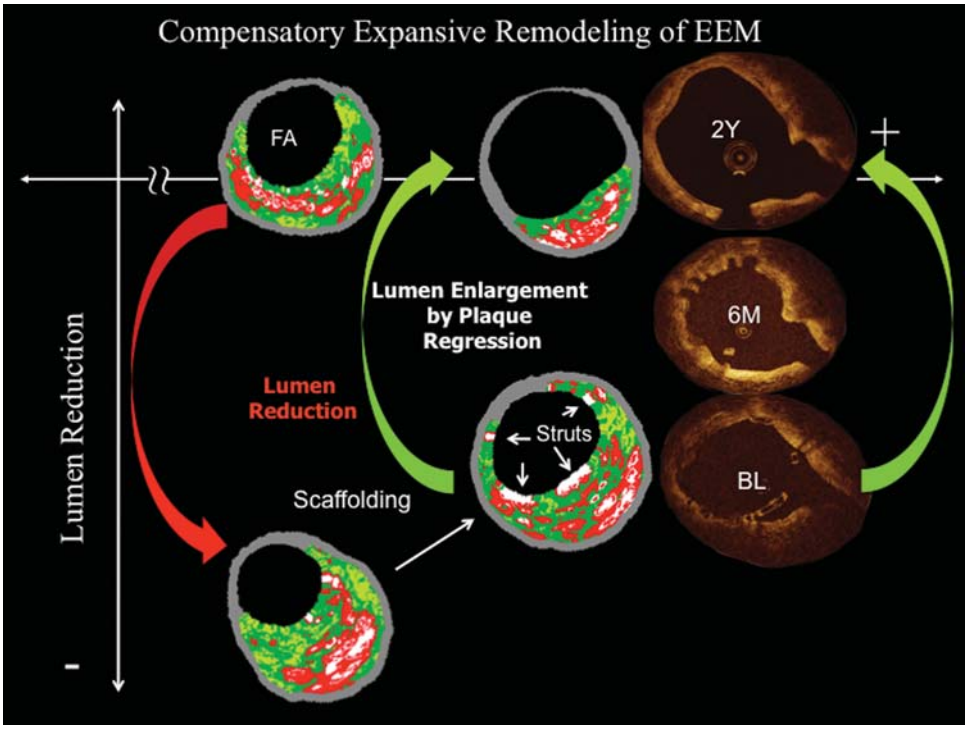

Figure 3 The atherosclerotic process is characterized by a lumen reduction (vertical axis) associated with remodelling (horizontal axis) of the vessel wall. If treated with bioresorbable scaffold, the lumen will get enlarged at long term. Late evolutional events are fully described in the text.

The initially compensatory remodelling of the vessel wall tends to accommodate plaque growth, in order to maintain the patency of the vessel lumen. At a certain level, characterized by a plaque burden of more or less 40%, the lumen reduction becomes irremediable.[34] When the stenotic lesion becomes flow limiting, surgical or percutaneous treatment of the vessel blockage, to alleviate the ischaemic manifestation, become unavoidable.

Transluminal dilatation of the stenotic lesion was introduced by Andreas Gruentzig as an alternative to the bypass treatment of the flow-limiting stenosis, but as described above, it was only a first step in the modern history of PCI. Nowadays, when the therapeutic decision is made to dilate flow-limited lesion(s), it implies *de facto* the implantation of a BMS or drug-eluting metal stent in vessels that will be forever caged by this permanent metallic implants.

One possible fate of the dilated but caged lesion is an intra-stent lumen reduction by intra-stent neointimal tissue growth, even if the cytostatic drug slows down or postpones the phenomenon. This neointimal tissue may in turn degenerate and become atherosclerotic, up to the point where it will develop its own vulnerable plaque and rupture inside the cage of the stent.[36] The recent publication by Nakazawa *et al.*[37] has emphasized that process, and *in vivo* OCT images of intra-stent plaque ruptures have been documented (*Figure 2*).

It is suspected that cytostatic and cytotoxic drugs may profoundly alter the metabolism of the vessel wall, weaken its structure, and ultimately effect a retraction of the surrounding vessel wall from the metallic cage, generating late acquired malapposition. It has been demonstrated that a large malapposition at baseline will also persist at long term. Late and very late stent thrombosis has been associated with late malapposition, either acquired or persistent.[18]

In both scenarios, the intravascular cage interferes with the natural biological dynamism of the vessel wall. Presumably, biology, pharmacology, and physiology are impeded by the presence of this permanent metallic cage. Prior to frank-acquired malapposition, minor signs of interaction between the dynamism of the vessel wall and the DES can be detected by OCT and a varied vocabulary has been used to describe the ballooning effect of the lumen vessel wall between the struts creating initially a crenated appearance of the vessel, sometimes casually termed a 'cauliflower' appearance. That phenomenon can be so intense that the vessel wall will ultimately get detached from the tethering struts, which will permanently remain isolated in the middle of the flowing blood[38,39] (*Figure 2*).

. . .To a transient bioresorbable scaffold

The change in paradigm with biodegradable scaffold is suggested by previous observations made with the first ABSORB generation.[24,40]

At 2 years, we observed and reported the complete bioresorption of the polymeric struts, which were no longer detectable by OCT, by intravascular ultrasound (IVUS) grey scale, and by IVUS-virtual histology (VH), confirming thereby preclinical studies.[28] The other critical observation made by IVUS between 6-month and 2-year follow-up was a late luminal enlargement (10.9%) with significant plaque media reduction (12.7%) and without significant change in the vessel wall area (EEM). Still today, it is unknown whether this 'plaque media regression' on IVUS is a true atherosclerotic regression, with change in vessel wall composition and plaque morphology (from thin-cap atheroma to thick-cap atheroma) or a pseudo-regression due to bioresorption of the polymeric struts.[41] True atherosclerotic regression could only be hypothesized based on animal and *in vitro* experiments, showing that mammalian target of rapamycin can trigger a complex chain of biological reactions that leads finally to activation of genes related to autophagy of macrophages.[42,43] During that process, the macrophage's cytoplasm becomes intensively vacuolized and exhibits autophagolysosomes containing various atherosclerotic debris (*Figure 4*). To what extent that process is involved in human plaque regression is unknown, but inhibition of $LPPLA_2$, which results in plaque area reduction and halts progression of the necrotic core, is another possible example of true atherosclerotic regression.[44]

Nevertheless, pseudo-regression is still a plausible alternative explanation.

In a very limited number of patients, VH imaging pre-scaffolding, post-scaffolding, and at 6 and 24 months were obtained, documenting post-treatment a sudden increase in plaque media, due to the artefactual implantation of 6 mm^3 of polymer (volume of polymeric material of a 3 mm diameter scaffold with a length of 18 mm) detected and misinterpreted by IVUS backscattering as dense calcium or hyperechogenic tissue. The subsequent 12% plaque area reduction documented between 6 and 24 months may be simply related to the actual disappearance of the struts (*Figure 5*).

A potential drawback or 'new enemy' of this new technology is strut fracture. Unlike metallic stents, the polymeric devices have inherent limits of expansion and can break as a result of over-dilatation. In an anecdotal case from the ABSORB cohort A, a 3.0 mm scaffold was over-expanded with 3.5 mm balloon, which resulted in strut fracture as documented with OCT. Due to the recurrence of limited anginal symptoms, this patient underwent target lesion revascularization, despite an angiographically non-significant stenosis by quantitative coronary angiography (%DS of 42%). The clinical significance of such a case, only evidenced by OCT, needs to be further elucidated, but undoubtedly stent fracture should be avoided by respecting the nominal size of the scaffold.

Other biological implications of a metallic stent vs. bioresorbable scaffold

There are other more complex biological interferences resulting from metallic caging. In the BMS era, our group and others have shown that stiff metallic stents can alter vessel geometry and biomechanics and that long-term flow disturbances and chronic irritation contribute to adverse events, without mentioning late strut fractures, that could lead to restenosis and clinical events.[45–48] In these studies, after metallic stent implantation,

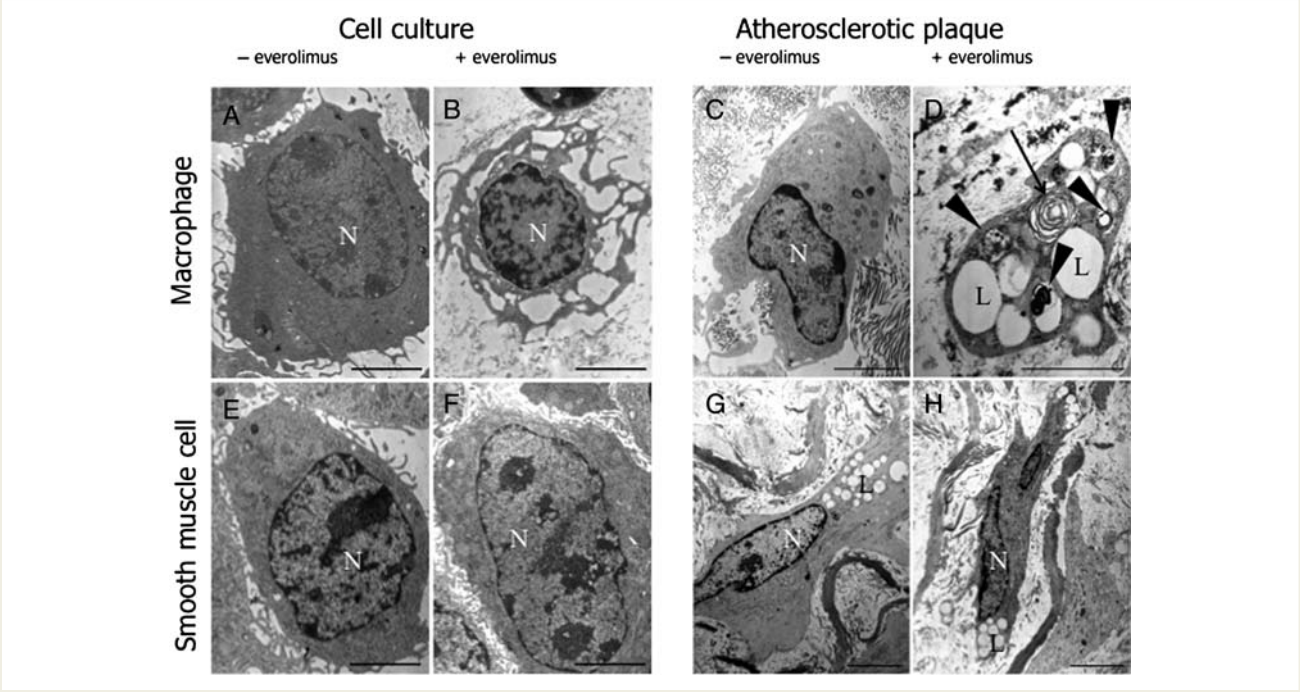

Figure 4 Ultrastructural features of a normal mouse macrophage (*A* and *C*) and smooth muscle cells (*E* and *G*) as an untreated control with normal cell morphology (modified from Verheye *et al.*[43]) In cell culture, treatment of macrophages with everolimus (10 μmol/L) showing different stages of autophagic cell death, which was characterized by cell shrinkage, extensive vacuolization, depletion of organelles, and presence of an intact, non-pyknotic nucleus (*B*). In atherosclerotic plaque, *in vitro* treatment of these atherosclerotic plaques with everolimus (10 μmol/L) for 3 days also resulted in autophagic cell death and was also characterized by cell shrinkage, depletion of organelles, and presence of large autophagosomes containing membranous whorls and remnants of cytoplasmatic material. (*D*). Autophagy was not induced in everolimus-treated (10 μmol/L) smooth muscle cell (*F* and *H*).[43] Arrowheads, autophagy vesicles; arrow, myelin figure; L, lipid droplet; N, nucleus.

the curvature increased by 121% at the entrance and by 100% at the exit of the stent, resulting in local changes in shear stress correlated with the local curvature (*Figure 6*). Stent implantation changed three-dimensional (3D) vessel geometry in such a way that regions with decreased and increased shear stress emerged close to the stent edges. These changes were related to the asymmetric patterns of in-stent restenosis.[45] From that point of view, the initial superior conformability and flexibility of the ABSORB with respect to metallic stents (Multilink Vision) can, at an early stage, contribute to less change in vessel geometry and biomechanics (*Figure 7*).[48] Late strut fracture should not be an issue, since at late time points, the struts have disappeared.

Not only change in curvature but also mismatch in area/diameter (step-up, proximal edge of the stent; step-down, distal edge of the stent) may generate oscillatory shear stress, which gives rise to the expression of several growth factors.[49]

With BMSs, we demonstrated that neointimal thickness was at 6 months inversely related to the relative shear stress distribution. Subsequently, we studied the impact of the shear stress pattern (obtained from computational fluid dynamic calculations) on the true 3D neointimal thickness distribution in sirolimus-eluting stents in coronary arteries. Small pits were observed between the stent struts; deeper pits were present on the outside curvature of the stented segments. In regions of low or even oscillatory shear stress, distal to the endoluminal protrusion of the strut, it is hypothesized that prolonged tissue contact and retention of the cytostatic drugs within the vessel wall could affect the metabolism of the vessel wall tissue, resulting in the crenated appearance of the vessel wall between the struts[50] (*Figure 8*).

Mechanical conditioning, renewed compliance, dynamic vasomotion, and mechanotransduction: the tenet of vascular reparative therapy

Using palpography, we have demonstrated that the scaffolding properties of the bioresorbable polymer offer the advantages of gradual load transfer of mechanical strain to the healing tissue (mechanical conditioning) (strain values: post-procedure, 0.16 ± 0.10; 6 months, 0.28 ± 0.12; 2 years, 0.31 ± 0.17%)[24] so that the healthy compliance of the vessel can be progressively restored long term (renewed compliance). Gradual exposure of cellular structures within the vessel wall to normal physiological stress conditions has a positive effect on cellular organization and function. In the field of orthopaedic biodegradable implants, mechanical conditioning via progressive dynamic loading improves proteoglycan and collagen deposition.[51] A similar scenario has been

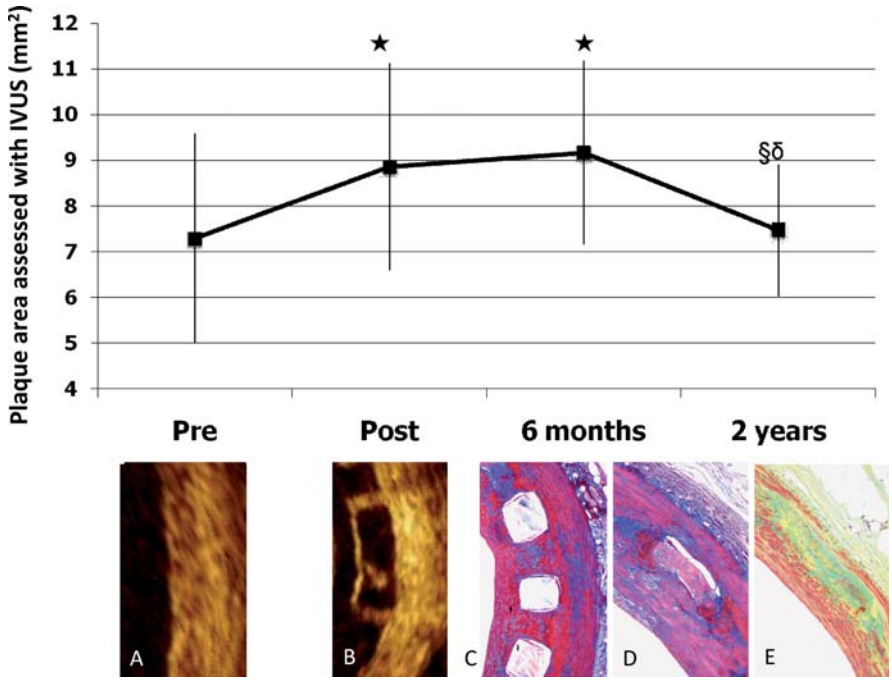

Figure 5 (Upper panel) Average plaque area (black dot) and its standard deviation (vertical bar) in the subset of patients with pre-stenting, post-stenting, 6 months, and 2-year follow-up. $^{\star}P < 0.05$ vs. pre-stenting, $^{\S}P < 0.005$ vs. 6 months, and $^{\delta}P < 0.05$ vs. post-stenting.[41] (Lower panel) Optical coherence tomography image before (*A*) and immediately after scaffold implantation (*B*), in a porcine coronary model. Histology images with trichrome staining show initially neointimal hyperplasia between and on top of the struts (*C*). At medium term, the void previously occupied by the polymeric material becomes filled with connective tissue. At long term, the strut voids become undetectable in histology (Movat's staining), with vessel wall thinning (*E*).[59]

deciphered with vascular bioresorbable implants. After bioresorption of the polylactide, the void previously occupied by the struts is filled progressively by proteoglycan and collagen (*Figure 4*). The full disappearance of the struts—which has been documented by ultrasound, OCT, histology, and pharmacologically induced dynamic vasomotion—suggested that the vessel wall will ultimately sense again the mechanical strains of pulsatile blood flow (pulsatility), which is an important stimulus for the cell biology of the vessel wall[24] (*Figure 9*).

Pulsatility is the fluctuation of blood pressure and blood flow velocity during systole and diastole. As blood is pumped through the coronary vessels, the vessel wall is exposed to two sets of forces, both of which are critically important: (i) shear stress is the frictional force on the vessel lining as blood flows through it, (ii) cyclic strain is the force generated by the stretching of the vessel wall during systole and is affected by vessel distensibility (stretchability), and (iii) the interplay of shear stress and cyclic strain controls cell signalling—the chemical signals sent from one cell to another, which can lead to atheroprotective/thromboresistant changes, or disease progression and instability. For instance, cyclic strain stimulates eNOS gene regulation and steady-state levels of prostacyclin are significantly increased if the shear stress force is applied in a pulsatile fashion compared with steady laminar flow.[52,53] Cell signalling may be altered in stented segments, where the vessel distensibility is eliminated by metallic caging of the vessel segment. The translation of mechanical forces into chemical signals by cells is referred to as 'mechanotransduction'.

Applied mechanical strain preferentially preserves collagen fibrils, and stretch of the vascular wall stimulates increased actin polymerization, activating the synthesis of smooth muscle-specific proteins. Under such conditions, smooth muscle cells preferentially maintain their contractile phenotype, while such differentiation is lost in sites of vascular injury (i.e. atherosclerosis or restenosis). From that point of view, the transmission microscopy of neointima and media, at 1 and 36 months in pigs having received ABSORB, is very illustrative of the changes in phenotype observed the short- and long term in these vessels (*Figure 9*).

In summary, with the progressive disappearance of the polymeric scaffold, physiological stimuli can again have an active impact on the vessel wall, and the return of pulsatility may be of paramount importance in effecting optimal repair of the vessel wall.

In our patients treated with BRS, vasomotion of the scaffolded segment following intraluminal administration of acetylcholine[30,54] suggests that: (i) the scaffolding function of the polymeric struts has completely disappeared and the so-called scaffolded segment can now exhibit vasomotion, (ii) the endothelial lining (coverage) is coalescent, (iii) the ciliary function of the endothelial cell is functional, and (iv) the biochemical process through which nitric oxide is released properly works. A positive acetylcholine test with vasodilatation of the scaffold is the indirect proof that the endothelium is anatomically and functionally normal and healthy. In a porcine

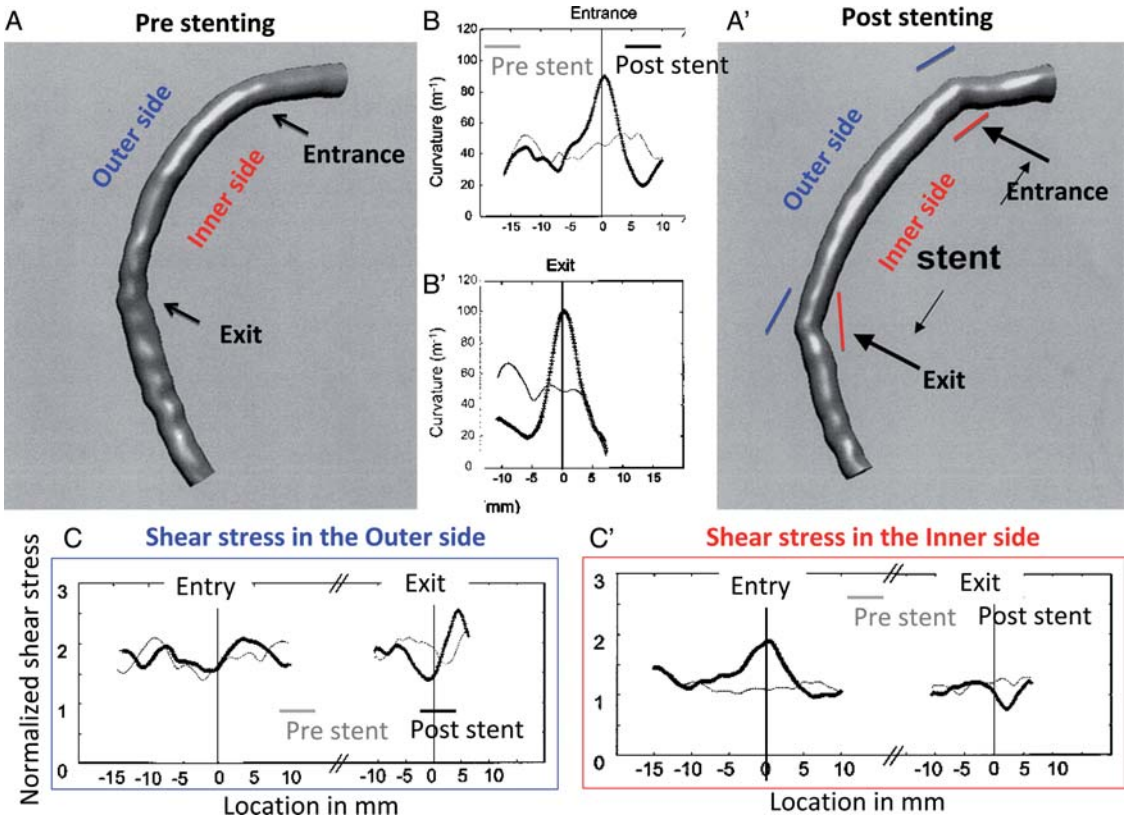

Figure 6 (*A* and *A*′) Three-dimensional reconstruction of a right coronary artery in a porcine model pre- (*A*) and after (*A*′) metallic stent implantation. (*B* and *B*′) Average curvature of the arteries relative to the location of the entrance (0 mm in *B*) and exit of the stent (0 mm in *B*′) before (grey) and after (black) stent implantation. (*C* and *C*′) Average normalized shear stress relative to the location of the entrance (0 mm) and exit of the stent (0 mm) before (grey) and after (black) stent implantation in the inner curve (*C*) and outer curve (*C*′). Location sign: distal is positive. Modified from Wentzel *et al.*[45]

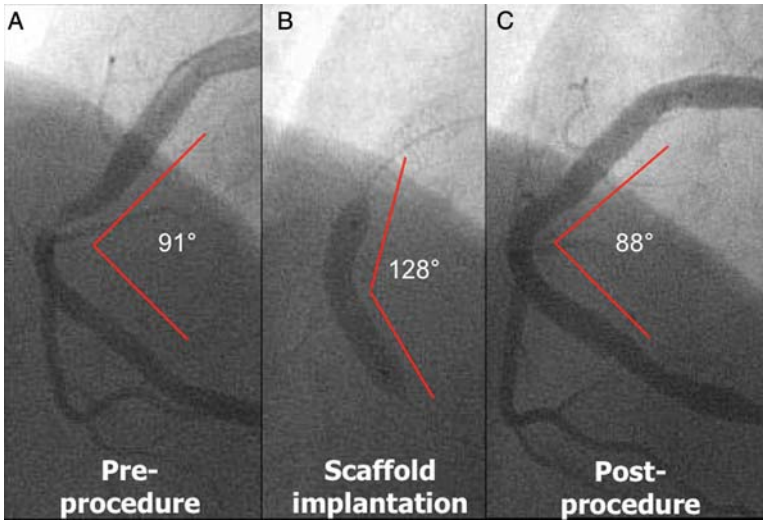

Figure 7 Angiogram of the right coronary artery pre-treatment (*A*), and post-implantation of bioresorbable scaffold (*C*). In-between, cine-filming of the delivery system during full inflation of the balloon (*B*). Note that the initial angulation of 91° widened to 128° during device delivery, to come back to 88° after implantation of the scaffold and removal of the balloon.

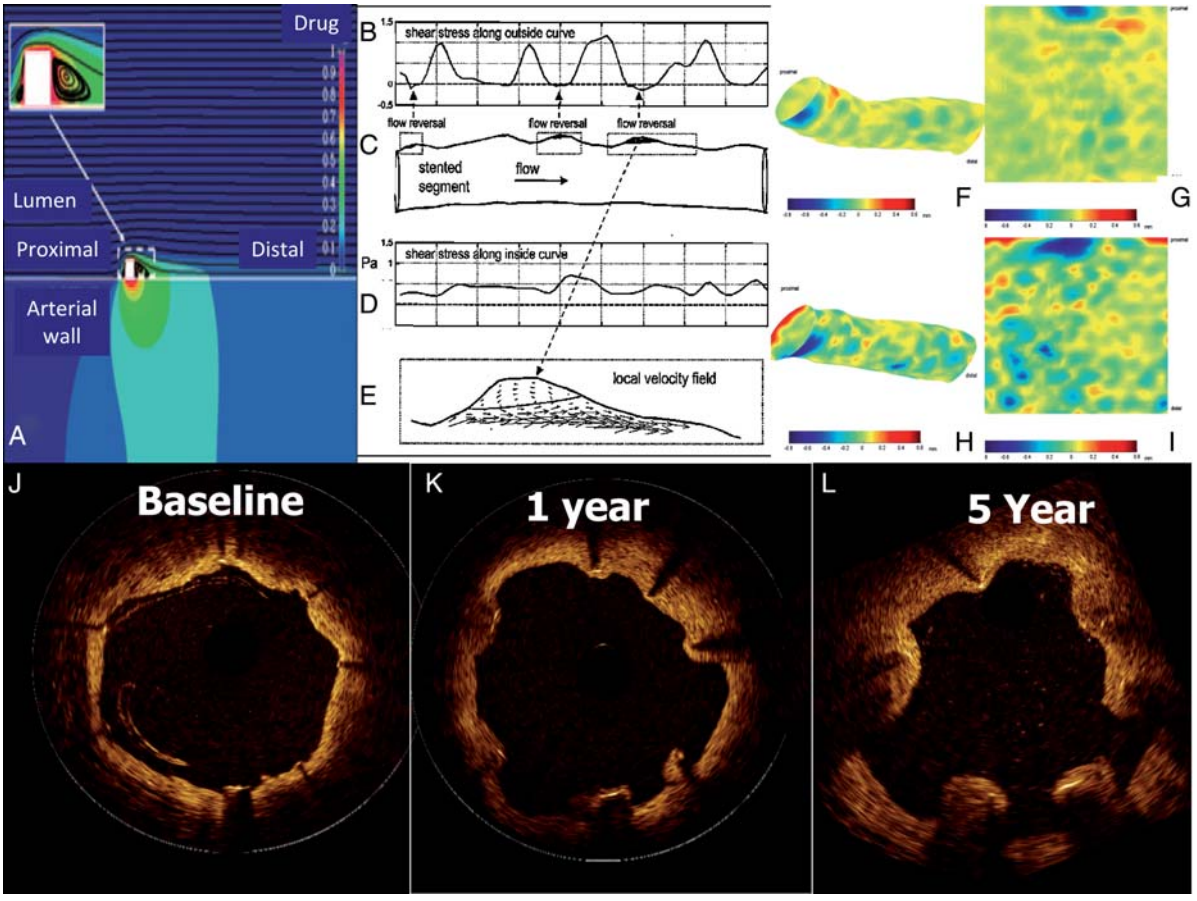

Figure 8 (*A*) A single drug-eluting stent strut. Visual representation of drug concentration distribution (in colour) and blood flow profiles (black curves). (Inset) High magnification of area outlined by white dashed line (reprinted from Balakrishnan *et al.*).[65] (*C*) Two-dimensional axial cross-section of a slightly curved stented segment with a sirolimus-eluting stent. The results of a computation of velocity and shear stress distribution in this segment at follow-up show regions with low shear stress (*B*) that coincide with the shallow pits in (*C*). Along the inner curve, the region with lower shear stress, the pits are virtually absent and shear stress distribution is much more homogeneous (*D*). In some of the pits along the outside curve, flow reversal can be observed (inset and *E*). The areas containing negative axial velocity are indicated by the shaded boxed regions in (*C*).[66] (*F–I*) Local intimal thickness colour-coded and projected on the sirolimus-eluting stent surface. The colour code indicates the relative position of lumen surface to the stent surface ranging from −0.8 mm (blue) to 0.6 mm (red). (*F* and *H*) The three-dimensional-reconstructed images after the procedure and at follow-up, respectively. (*G* and *I*) The unfolded carpet view of (*F*) and (*H*), respectively. The images at follow-up (*H* and *I*) identify additional blue areas, indicating disappearance of tissue between stent struts and lumen enlargement. Localized neointimal hyperplasia (red area) was also observed.[67] (*J–L*) Serial optical coherence tomography cross-sectional images immediately, 1 and 5 years after implantation of sirolimus-eluting stent. The slight tissue prolapses between the struts seen at baseline are at 1 year replaced by crenated appearance of the endoluminal lining. At 5 years, the vessel wall gets detached from the struts, which will permanently remain isolated in middle of flowing blood (by courtesy of Lorenz Räber and Maria Radu).

model, transmission electron microscopy shows the sign of maturation of endothelial junctions between 1 and 36 months with a robust and dense intercellular desmosome at 3 years. Of note, a healthy endothelium releases chemical signals that promote vasodilation (NO), inhibit thrombosis (prostacyclin, tissue plasminogen activator, thrombomodulin), inhibit smooth muscle cell proliferation, and inhibit inflammation. Conversely, an unhealthy endothelium releases chemical signals that promote vasoconstriction (endothelin, angiotensin II, thromboxane A2), thrombosis (von Willebrand factor, fibrinogen, tissue factor, plasminogen activator inhibitor, thromboxane A2), disease progression (vascular endothelial growth factor, platelet-derived growth factor), and inflammation (vascular cell adhesion molecules, intercellular adhesion molecule).[55]

As mentioned above, late lumen enlargement was not associated with vessel enlargement, and thus was obtained through a reduction in plaque area.[24] A few hypothetical mechanisms can be put forward to explain this phenomenon. First, everolimus may significantly lower monocyte chemotaxis, without inducing monocyte cell death by affecting chemotactic factors such as monocyte chemoattractant protein 1, fractalkine, interleukin-8, and *N*-formyl-methionyl-leucyl-phenylalanine.[56] Secondly, the drug itself has been shown to reduce advanced and intermediate lesions in mice knockout for LDL receptor (−/−).[57] Thirdly,

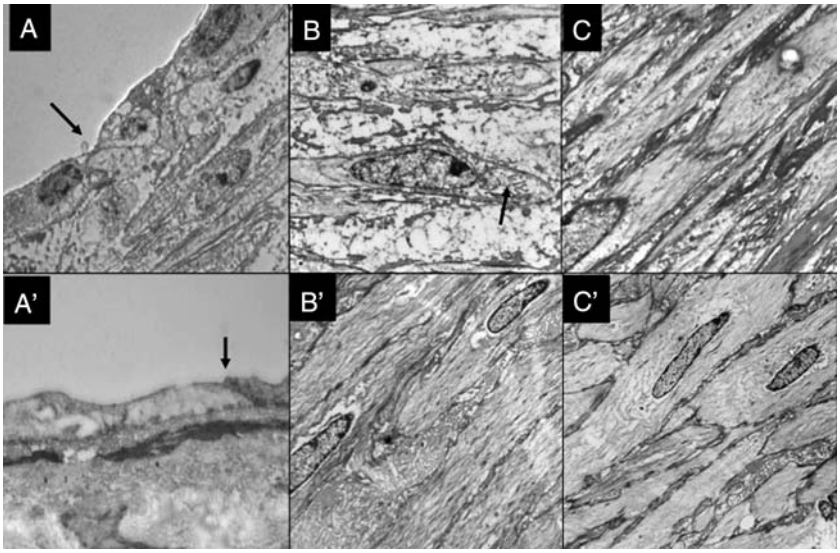

Figure 9 Transmission electron microscopic images of endothelium (*A* and *A′*), neointima (*B* and *B′*), and media (*C* and *C′*) in a porcine model implantation at 1 month (*A*–*C*) and at 36 months (*A′*–*C′*) after bioresorbable scaffold implantation. At 1 month, transmission electron microscopy of the endothelium shows a single, weak junctions (arrow in *A*), while at 36 months, transmission electron microscopy shows overlaying endothelial cells with dense continuous junctions (*A′*). Neointima at 1 month shows intra-cytoplasmic organelle in smooth muscle cells with secretive phenotype (*B*), while at 36 months transmission electron microscopy shows in the neointima smooth muscle cells rich in actin fibre with a typical contractile phenotype (*B′*). The contractile phenotype of smooth muscle cells in the media remains unchanged between one (*C*) and 36 months (*C′*). Modified from Vorpahl *et al.*[68]

everolimus has been shown to selectively clear macrophages in plaque by inducing autophagy in animal models (see above). This could result in a reduction in plaque volume. Fourthly, pulsatile laminar flow may trigger plaque regression, through stimulation of matrix metalloproteinases.[58]

Imaging of vascular reparative therapy

The actual cross-sections figuring in the schematic illustration are real cross-sections of a patient treated with ABSORB (1.0). The sequence of events showed that the necrotic core in direct contact with the lumen (thin-cap atheroma) did regress at 2 years, and the remaining necrotic core became isolated from the lumen by a *de novo* fibrotic layer/cap (thick-cap atheroma). The central cross-sectional VH image (*Figure 3*) shows the enlargement of the original flow-limiting lesion, due to the deployment of the BRS (the polymeric struts are identified on VH as small blocks of pseudo-dense calcium). At 2 years, full resolution of the pseudo-VH images of calcium and OCT disappearance of the polymeric struts confirmed the complete resorption and integration of the bioprosthesis (ABSORB 1.0) into the vessel wall.[59] At that stage, the transiently scaffolded vessel is no longer caged (as it would be by a permanent metallic stent structure) and we may surmize that physiological stimulus, such as shear stress as well as pharmacological action of new anti-inflammatory drugs or drugs capable of reversing the cholesterol transport, could now act freely on the vessel wall and result in further enlargement of the lumen vessel not hindered by permanent metallic boundaries.[44,60] In conjunction with the return of the vasomotion, it is appealing to name the entire process vascular reparative therapy.[24,61] However, calcified plaque, the ultimate remnant after cell death, will have to be removed mechanically or by some kind of osteoclastic biological process, currently inexistent in our vascular pharmacological armamentarium.[62]

This kind of vessel transiently scaffolded by a BRS, now fully amenable to biological, pharmacological, and physiological impact, may allow a more permissive and extensive paving of large areas of atherosclerosis in order to reduce cardiac morbidity and mortality associated with plaque rupture.[63,64] This hypothetical scheme may herald a change in paradigm moving from what currently is a permanently scaffolded metal–tissue composite doomed to caging and lumen loss to a future repaired vessel with late enlargement of the lumen, freed after scaffold resorption, and responding to its biological environment.

Conflict of interest: none declared.

References

1. European perspectives. *Circulation* 2010;**121**:f1–f6.
2. Gruntzig A. Transluminal dilatation of coronary-artery stenosis. *Lancet* 1978;**1**:263.
3. Ormiston JA, Stewart FM, Roche AH, Webber BJ, Whitlock RM, Webster MW. Late regression of the dilated site after coronary angioplasty: a 5-year quantitative angiographic study. *Circulation* 1997;**96**:468–474.
4. Sigwart U, Puel J, Mirkovitch V, Joffre F, Kappenberger L. Intravascular stents to prevent occlusion and restenosis after transluminal angioplasty. *N Engl J Med* 1987;**316**:701–706.

5. Roubin GS, Cannon AD, Agrawal SK, Macander PJ, Dean LS, Baxley WA, Breland J. Intracoronary stenting for acute and threatened closure complicating percutaneous transluminal coronary angioplasty. *Circulation* 1992;**85**:916–927.
6. Schatz RA, Baim DS, Leon M, Ellis SG, Goldberg S, Hirshfeld JW, Cleman MW, Cabin HS, Walker C, Stagg J. Clinical experience with the Palmaz-Schatz coronary stent. Initial results of a multicenter study. *Circulation* 1991;**83**:148–161.
7. Serruys PW, Keane D. The bailout stent. Is a friend in need always a friend indeed? *Circulation* 1993;**88**(5 Pt 1):2455–2457.
8. Schwartz RS, Topol EJ, Serruys PW, Sangiorgi G, Holmes DR Jr. Artery size, neointima, and remodeling: time for some standards. *J Am Coll Cardiol* 1998;**32**: 2087–2094.
9. Garg S, Serruys PW. Coronary stents: current status. *J Am Coll Cardiol* 2010; **56**(Suppl. 10):S1–S42.
10. Serruys PW, de Jaegere P, Kiemeneij F, Macaya C, Rutsch W, Heyndrickx G, Emanuelsson H, Marco J, Legrand V, Materne P, Belardi J, Sigwart U, Colombo A, Goy JJ, van den Heuvel P, Delcan J, Morel M-a. A comparison of balloon-expandable-stent implantation with balloon angioplasty in patients with coronary artery disease. Benestent Study Group. *N Engl J Med* 1994;**331**: 489–495.
11. Fischman DL, Leon MB, Baim DS, Schatz RA, Savage MP, Penn I, Detre K, Veltri L, Ricci D, Nobuyoshi M, Cleman M, Heuser R, Almond D, Teirstein PS, Fish RD, Colombo A, Brinker J, Moses J, Shaknovich A, Hirshfeld J, Bailey S, Ellis S, Rake R, Goldberg S. A randomized comparison of coronary-stent placement and balloon angioplasty in the treatment of coronary artery disease. Stent Restenosis Study Investigators. *N Engl J Med* 1994;**331**:496–501.
12. Serruys PW, Strauss BH, Beatt KJ, Bertrand ME, Puel J, Rickards AF, Meier B, Goy JJ, Vogt P, Kappenberger L, Sigwart U. Angiographic follow-up after placement of a self-expanding coronary-artery stent. *N Engl J Med* 1991;**324**:13–17.
13. Sousa JE, Costa MA, Abizaid A, Abizaid AS, Feres F, Pinto IM, Seixas AC, Staico R, Mattos LA, Sousa AG, Falotico R, Jaeger J, Popma JJ, Serruys PW. Lack of neointimal proliferation after implantation of sirolimus-coated stents in human coronary arteries: a quantitative coronary angiography and three-dimensional intravascular ultrasound study. *Circulation* 2001;**103**:192–195.
14. Rensing BJ, Vos J, Smits PC, Foley DP, van den Brand MJ, van der Giessen WJ, de Feijter PJ, Serruys PW. Coronary restenosis elimination with a sirolimus eluting stent: first European human experience with 6-month angiographic and intravascular ultrasonic follow-up. *Eur Heart J* 2001;**22**:2125–2130.
15. Morice MC, Serruys PW, Sousa JE, Fajadet J, Ban Hayashi E, Perin M, Colombo A, Schuler G, Barragan P, Guagliumi G, Molnar F, Falotico R. A randomized comparison of a sirolimus-eluting stent with a standard stent for coronary revascularization. *N Engl J Med* 2002;**346**:1773–1780.
16. Finn AV, Joner M, Nakazawa G, Kolodgie F, Newell J, John MC, Gold HK, Virmani R. Pathological correlates of late drug-eluting stent thrombosis: strut coverage as a marker of endothelialization. *Circulation* 2007;**115**:2435–2441.
17. Joner M, Finn AV, Farb A, Mont EK, Kolodgie FD, Ladich E, Kutys R, Skorija K, Gold HK, Virmani R. Pathology of drug-eluting stents in humans: delayed healing and late thrombotic risk. *J Am Coll Cardiol* 2006;**48**:193–202.
18. Cook S, Ladich E, Nakazawa G, Eshtehardi P, Neidhart M, Vogel R, Togni M, Wenaweser P, Billinger M, Seiler C, Gay S, Meier B, Pichler WJ, Juni P, Virmani R, Windecker S. Correlation of intravascular ultrasound findings with histopathological analysis of thrombus aspirates in patients with very late drug-eluting stent thrombosis. *Circulation* 2009;**120**:391–399.
19. Waksman R. Biodegradable stents: they do their job and disappear. *J Invasive Cardiol* 2006;**18**:70–74.
20. Stack RS, Califf RM, Phillips HR, Pryor DB, Quigley PJ, Bauman RP, Tcheng JE, Greenfield JC Jr. Interventional cardiac catheterization at Duke Medical Center. *Am J Cardiol* 1988;**62**(10 Pt 2):3F–24F.
21. Babalik E, Gulbaran M, Gurmen T, Ozturk S. Fracture of popliteal artery stents. *Circ J* 2003;**67**:643–645.
22. Okamura T, Serruys PW, Regar E. Three-dimensional visualization of intracoronary thrombus during stent implantation using the second generation, Fourier domain optical coherence tomography. *Eur Heart J* 2010;**31**:625.
23. Eggebrecht H, Rodermann J, Hunold P, Schmermund A, Bose D, Haude M, Erbel R. Images in cardiovascular medicine. Novel magnetic resonance-compatible coronary stent: the absorbable magnesium-alloy stent. *Circulation* 2005;**112**:e303–e304.
24. Serruys PW, Ormiston JA, Onuma Y, Regar E, Gonzalo N, Garcia-Garcia HM, Nieman K, Bruining N, Dorange C, Miquel-Hebert K, Veldhof S, Webster M, Thuesen L, Dudek D. A bioabsorbable everolimus-eluting coronary stent system (ABSORB): 2-year outcomes and results from multiple imaging methods. *Lancet* 2009;**373**:897–910.
25. van der Giessen WJ, Slager CJ, van Beusekom HM, van Ingen Schenau DS, Huijts RA, Schuurbiers JC, de Klein WJ, Serruys PW, Verdouw PD. Development of a polymer endovascular prosthesis and its implantation in porcine arteries. *J Interv Cardiol* 1992;**5**:175–185.
26. Tamai H, Igaki K, Kyo E, Kosuga K, Kawashima A, Matsui S, Komori H, Tsuji T, Motohara S, Uehata H. Initial and 6-month results of biodegradable poly-L-lactic acid coronary stents in humans. *Circulation* 2000;**102**:399–404.
27. Onuma Y, Garg S, Okamura T, Ligthart J, van Geuns RJ, de Feijter PJ, Serruys PW, Tamai H. Ten-year follow-up of the Igaki-Tamai stent a posthumous tribute to the scientific work of Dr. Hideo Tamai. *EuroIntervention* 2010;**5**(Suppl. F):F109–F111.
28. Onuma Y, Serruys P, Perkins L, Okamura T, Gonzalo N, Garcia-Garcia HM, Regar E, Kamberi M, Powers JC, Rapoza R, van Beusekom H, van der Giessen W, Virmani R. Intracoronary optical coherence tomography (OCT) and histology at 1 month, at 2, 3 and 4 years after implantation of everolimus-eluting bioresorbable vascular scaffolds in a porcine coronary artery model: an attempt to decipher the human OCT images in the ABSORB trial. *Circulation* 2010 (in press).
29. Tsuji T, Tamai H, Igaki K, Hsu Y-S, Kosuga K, Hata T, OKada M, Nakamura T, Fujita S. Four-year follow-up of the biodegradable stent (IGAKI-TAMAI Stent). *Circ J* 2004;**68**(Suppl. 1):135.
30. Ormiston JA, Serruys PW, Regar E, Dudek D, Thuesen L, Webster MW, Onuma Y, Garcia-Garcia HM, McGreevy R, Veldhof S. A bioabsorbable everolimus-eluting coronary stent system for patients with single de-novo coronary artery lesions (ABSORB): a prospective open-label trial. *Lancet* 2008;**371**: 899–907.
31. Serruys PW, Onuma Y, Ormiston JA, de Bruyne B, Regar E, Dudek D, Thuesen L, Smits PC, Chevalier B, McClean D, Koolen J, Windecker S, Whitbourn R, Meredith I, Dorange C, Veldhof S, Miquel-Hebert K, Rapoza R, Garcia-Garcia HM. Evaluation of the second generation of a bioresorbable everolimus drug-eluting vascular scaffold for treatment of de novo coronary artery stenosis: six-month clinical and imaging outcomes. *Circulation* 2010;**122**: 2301–2312.
32. Erbel R, Di Mario C, Bartunek J, Bonnier J, de Bruyne B, Eberli FR, Erne P, Haude M, Heublein B, Horrigan M, Ilsley C, Bose D, Koolen J, Luscher TF, Weissman N, Waksman R. Temporary scaffolding of coronary arteries with bioabsorbable magnesium stents: a prospective, non-randomised multicentre trial. *Lancet* 2007;**369**:1869–1875.
33. Onuma Y, Serruys PW. Bioresorbable scaffold: the advent of a new era in percutaneous coronary and peripheral revascularization? *Circulation* 2011;**123**:779–797.
34. Glagov S, Bassiouny HS, Sakaguchi Y, Goudet CA, Vito RP. Mechanical determinants of plaque modeling, remodeling and disruption. *Atherosclerosis* 1997; **131**(Suppl.):S13–S14.
35. Kolodgie FD, Burke AP, Nakazawa G, Virmani R. Is pathologic intimal thickening the key to understanding early plaque progression in human atherosclerotic disease? *Arterioscler Thromb Vasc Biol* 2007;**27**:986–989.
36. Ramcharitar S, Garcia-Garcia HM, Nakazawa G, Kukreja N, Ligthart J, Virmani R, Serruys PW. Ultrasonic and pathological evidence of a neo-intimal plaque rupture in patients with bare metal stents. *EuroIntervention* 2007;**3**:290–291.
37. Nakazawa G, Otsuka F, Nakano M, Vorpahl M, Yazdani SK, Ladich E, Kolodgie FD, Finn AV, Virmani R. The pathology of neoatherosclerosis in human coronary implants bare-metal and drug-eluting stents. *J Am Coll Cardiol* 2011;**57**:1314–1322.
38. Radu M, Jorgensen E, Kelbaek H, Helqvist S, Skovgaard L, Saunamaki K. Strut apposition after coronary stent implantation visualised with optical coherence tomography. *EuroIntervention* 2010;**6**:86–93.
39. Ozaki Y, Okumura M, Ismail TF, Naruse H, Hattori K, Kan S, Ishikawa M, Kawai T, Takagi Y, Ishii J, Prati F, Serruys PW. The fate of incomplete stent apposition with drug-eluting stents: an optical coherence tomography-based natural history study. *Eur Heart J* 2010;**31**:1470–1476.
40. Ormiston JA, Webster MW, Armstrong G. First-in-human implantation of a fully bioabsorbable drug-eluting stent: the BVS poly-L-lactic acid everolimus-eluting coronary stent. *Catheter Cardiovasc Interv* 2007;**69**:128–131.
41. Sarno G, Onuma Y, Garcia Garcia HM, Garg S, Regar E, Thuesen L, Dudek D, Veldhof S, Dorange C, Ormiston JA, Serruys PW. IVUS radiofrequency analysis in the evaluation of the polymeric struts of the bioabsorbable everolimus-eluting device during the bioabsorption process. *Catheter Cardiovasc Interv* 2010;**75**: 914–918.
42. Martinet W, Verheye S, De Meyer GR. Everolimus-induced mTOR inhibition selectively depletes macrophages in atherosclerotic plaques by autophagy. *Autophagy* 2007;**3**:241–244.
43. Verheye S, Martinet W, Kockx MM, Knaapen MW, Salu K, Timmermans JP, Ellis JT, Kilpatrick DL, De Meyer GR. Selective clearance of macrophages in atherosclerotic plaques by autophagy. *J Am Coll Cardiol* 2007;**49**:706–715.
44. Serruys PW, Garcia-Garcia HM, Buszman P, Erne P, Verheye S, Aschermann M, Duckers H, Bleie O, Dudek D, Botker HE, von Birgelen C, D'Amico D, Hutchinson T, Zambanini A, Mastik F, van Es GA, van der Steen AF, Vince DG, Ganz P, Hamm CW, Wijns W, Zalewski A. Effects of the direct lipoprotein-associated phospholipase A(2) inhibitor darapladib on human coronary atherosclerotic plaque. *Circulation* 2008;**118**:1172–1182.

45. Wentzel JJ, Whelan DM, van der Giessen WJ, van Beusekom HM, Andhyiswara I, Serruys PW, Slager CJ, Krams R. Coronary stent implantation changes 3-D vessel geometry and 3-D shear stress distribution. *J Biomech* 2000;**33**:1287–1295.
46. Gyongyosi M, Yang P, Khorsand A, Glogar D. Longitudinal straightening effect of stents is an additional predictor for major adverse cardiac events. Austrian Wiktor Stent Study Group and European Paragon Stent Investigators. *J Am Coll Cardiol* 2000;**35**:1580–1589.
47. Gomez-Lara J, Brugaletta S, Diletti R, Garg S, Onuma Y, Gogas BD, van Geuns RJ, Dorange C, Veldhof S, Rapoza R, Whitbourn R, Windecker S, Garcia-Garcia HM, Regar E, Serruys PW. A comparative assessment by optical coherence tomography of the performance of the first and second generation of the everolimus-eluting bioresorbable vascular scaffolds. *Eur Heart J* 2011;**32**:294–304.
48. Gomez-Lara J, Garcia-Garcia HM, Onuma Y, Garg S, Regar E, De Bruyne B, Windecker S, McClean D, Thuesen L, Dudek D, Koolen J, Whitbourn R, Smits PC, Chevalier B, Dorange C, Veldhof S, Morel MA, de Vries T, Ormiston JA, Serruys PW. A comparison of the conformability of everolimus-eluting bioresorbable vascular scaffolds to metal platform coronary stents. *JACC Cardiovasc Interv* 2010;**3**:1190–1198.
49. Thury A, Wentzel JJ, Vinke RV, Gijsen FJ, Schuurbiers JC, Krams R, de Feyter PJ, Serruys PW, Slager CJ. Images in cardiovascular medicine. Focal in-stent restenosis near step-up: roles of low and oscillating shear stress? *Circulation* 2002;**105**: e185–e187.
50. Cheng C, Tempel D, Oostlander A, Helderman F, Gijsen F, Wentzel J, van Haperen R, Haitsma DB, Serruys PW, van der Steen AF, de Crom R, Krams R. Rapamycin modulates the eNOS vs. shear stress relationship. *Cardiovasc Res* 2008;**78**:123–129.
51. Ciccone WJ 2nd, Motz C, Bentley C, Tasto JP. Bioabsorbable implants in orthopaedics: new developments and clinical applications. *J Am Acad Orthop Surg* 2001;**9**: 280–288.
52. Resnick N, Yahav H, Shay-Salit A, Shushy M, Schubert S, Zilberman LC, Wofovitz E. Fluid shear stress and the vascular endothelium: for better and for worse. *Prog Biophys Mol Biol* 2003;**81**:177–199.
53. Slager CJ, Wentzel JJ, Gijsen FJ, Schuurbiers JC, van der Wal AC, van der Steen AF, Serruys PW. The role of shear stress in the generation of rupture-prone vulnerable plaques. *Nat Clin Pract Cardiovasc Med* 2005;**2**:401–407.
54. Serruys PW, Onuma Y, Dudek D, Smits PC, Koolen J, Chevalier B, Bruyne Bd, Thuesen L, McClean D, Geuns R-Jv, Windecker S, Whitbourn R, Meredith I, Dorange C, Veldhof S, Hebert KM, Sudhir K, Garcia-Garcia HM, Ormiston JA. Evaluation of the second generation of a bioresorbable everolimus-eluting vascular scaffold for the treatment of de novo coronary artery stenosis: 12-month clinical and imaging outcomes. *J Am Coll Cardiol* 2011;**58**:1578–1588.
55. Alberts B, Johnson A, Lewis J, Raff M, Roberts K, Walter P. *Molecular Biology of the Cell*, 4th ed. New York: Garland Science, 2002.
56. Cheng C, Noordeloos AM, Jeney V, Soares MP, Moll F, Pasterkamp G, Serruys PW, Duckers HJ. Heme oxygenase 1 determines atherosclerotic lesion progression into a vulnerable plaque. *Circulation* 2009;**119**:3017–3027.
57. Mueller MA, Beutner F, Teupser D, Ceglarek U, Thiery J. Prevention of atherosclerosis by the mTOR inhibitor everolimus in LDLR−/− mice despite severe hypercholesterolemia. *Atherosclerosis* 2008;**198**:39–48.
58. Lehoux S, Tedgui A. Cellular mechanics and gene expression in blood vessels. *J Biomech* 2003;**36**:631–643.
59. Onuma Y, Serruys PW, Perkins LE, Okamura T, Gonzalo N, Garcia-Garcia HM, Regar E, Kamberi M, Powers JC, Rapoza R, van Beusekom H, van der Giessen W, Virmani R. Intracoronary optical coherence tomography and histology at 1 month and 2, 3, and 4 years after implantation of everolimus-eluting bioresorbable vascular scaffolds in a porcine coronary artery model: an attempt to decipher the human optical coherence tomography images in the ABSORB trial. *Circulation* 2010;**122**:2288–2300.
60. Khera AV, Cuchel M, de la Llera-Moya M, Rodrigues A, Burke MF, Jafri K, French BC, Phillips JA, Mucksavage ML, Wilensky RL, Mohler ER, Rothblat GH, Rader DJ. Cholesterol efflux capacity, high-density lipoprotein function, and atherosclerosis. *N Engl J Med* 2011;**364**:127–135.
61. Serruys PW, Onuma Y, Ormiston JA, Bruyne Bd, Regar E, Dudek D, Thuesen L, Smits PC, Chevalier B, McClean D, Koolen J, Windecker S, Whitbourn R, Meredith I, Dorange C, Veldhof S, Hebert KM, Rapoza R, Garcia-Garcia HM. Evaluation of the second generation of a bioresorbable everolimus drug-eluting vascular scaffold for treatment of de novo coronary artery stenosis six-month clinical and imaging outcomes. *Circulation* 2010;**122**:2288–2300.
62. Wada T, McKee MD, Steitz S, Giachelli CM. Calcification of vascular smooth muscle cell cultures: inhibition by osteopontin. *Circ Res* 1999;**84**:166–178.
63. Slepian MJ. Polymeric endoluminal gel paving: therapeutic hydrogel barriers and sustained drug delivery depots for local arterial wall biomanipulation. *Semin Interv Cardiol* 1996;**1**:103–116.
64. Ramcharitar S, Gonzalo N, van Geuns RJ, Garcia-Garcia HM, Wykrzykowska JJ, Ligthart JM, Regar E, Serruys PW. First case of stenting of a vulnerable plaque in the SECRITT I trial-the dawn of a new era? *Nat Rev Cardiol* 2009;**6**: 374–378.
65. Balakrishnan B, Tzafriri AR, Seifert P, Groothuis A, Rogers C, Edelman ER. Strut position, blood flow, and drug deposition: implications for single and overlapping drug-eluting stents. *Circulation* 2005;**111**:2958–2965.
66. Gijsen FJ, Oortman RM, Wentzel JJ, Schuurbiers JC, Tanabe K, Degertekin M, Ligthart JM, Thury A, de Feyter PJ, Serruys PW, Slager CJ. Usefulness of shear stress pattern in predicting neointima distribution in sirolimus-eluting stents in coronary arteries. *Am J Cardiol* 2003;**92**:1325–1328.
67. Tanabe K, Gijsen FJ, Degertekin M, Ligthart JM, Oortman RM, Serruys PW, Slager CJ. Images in cardiovascular medicine. True three-dimensional reconstructed images showing lumen enlargement after sirolimus-eluting stent implantation. *Circulation* 2002;**106**:e179–e180.
68. Vorpahl M, Finn A, Nakano M, Virmani R. The bioabsorption process: tissue and cellular mechanisms and outcomes. *EuroIntervention* 2009;**5**(Suppl. F): F28–F35.